Growing Solitary Disturbance in a Baroclinic Boundary Current

ATSUSHI KUBOKAWA

Department of Geophysics, Faculty of Science, Tohoku University, Sendai, Japan

(Manuscript received 11 December 1987, in final form 8 August 1988)

ABSTRACT

Weakly nonlinear longwaves in a horizontally sheared current flowing along a longitudinal boundary in a two-layer ocean are investigated by using a quasi-geostrophic β-plane model. Under the assumptions that the depth ratio of two layers is small, the β effect is weak and the waves are almost stationary, we obtain a set of coupled equations similar to that derived previously by Kubokawa for a coastal current with a surface density front on an f-plane. This set of equations contains soliton and cnoidal wave solutions and allows baroclinic instability to occur.

Considering a perturbation around the marginally stable condition, we obtain an analytic solution of a growing solitary disturbance with an amplitude larger than a certain critical value in a linearly stable eastward current. This disturbance propagates eastward, and grows by a baroclinic energy conversion. A numerical computation on its further evolution shows that after the amplitude exceeds another certain critical value, the disturbance begins to propagate westward and to radiate Rossby waves. This Rossby wave radiation causes the disturbance to decay and the propagation speed approaches zero. Nonlinear evolution of linearly unstable waves in an eastward current is also briefly discussed. The theory is applied to the Kuroshio Current in a qualitative way.

1. Introduction

The nonlinear dynamics of disturbances in currents with horizontal shear is an important subject of physical oceanography, since oceanic currents are horizontally sheared in general and large amplitude waves are frequently observed. It is well known that weakly nonlinear longwaves in such currents are governed by the Korteweg-de Vries (KdV) equations or modified KdV equations (e.g., Long 1964; Redekopp 1977; Hukuda 1979; Flierl 1979; Weideman and Redekopp 1980). These equations contain solitary wave (soliton) solutions. Although the solitons are stable, many observed eddies in oceanic currents are unstable. The main cause of such an unstable nature can be attributed to baroclinic instability (e.g., Ikeda et al. 1984; Griffiths and Pearce 1985). The primary motive of the present paper is to extend the weakly nonlinear longwave theory to the case allowing baroclinic instability to occur.

A closely related work was done by Kubokawa (1988, referred to as K88 hereafter). Kubokawa investigated weakly nonlinear longwaves on a density-driven coastal current with a surface front, which is marginally stable or unstable to the instability found by Killworth et al. (1984), and derived a set of coupled evolution equations. The equation describing the movement of the surface front is a KdV equation with an extra term, and it was numerically shown that disturbances with amplitudes larger than a certain critical value can be amplified even if the current is linearly stable.

On the other hand, Yoon and Yasuda (1987) found, in their numerical experiment on the path of the Kuroshio south of Japan, that a baroclinic disturbance with a finite amplitude grows extracting the energy from the potential energy of the linearly stable basic current. This phenomenon seems to be the same one as that discussed by K88. However, since K88 assumed the existence of the surface front and the zero potential vorticity in the upper layer, the application of his theory is restricted to narrow currents which flow in the direction of propagation of Kelvin wave. In other words, his theory is not applicable to currents like the Kuroshio. Therefore, we reformulate the problem using a quasi-geostrophic β-plane model and show that the same dynamics can also be important in this system. Furthermore, we present an analytic solution of a growing disturbance in a linearly stable current, and discuss the effect of β on its evolution.

After the derivation of the coupled evolution equations in the next section, the linear stability and nonlinear wave solutions are examined in section 3. In section 4, we present an analytic solution of growing solitary disturbance, and we carry out a numerical computation on its further evolution. In section 5, the evolution of linearly unstable waves in an eastward current is briefly discussed. The theoretical results are compared with the experimental ones in Yoon and Yasuda (1987) in a qualitative way in section 6.

Corresponding author address: Dr. Atsushi Kubokawa, Physical Oceanography Laboratory, Dept. of Geophysics, Faculty of Science, Tohoku University, Sendai 980, Japan.

2. Formulation

a. Model and basic equations

It is assumed throughout that quasi-geostrophic dynamics is applicable, and that the model ocean has the two-layer density structure shown in Fig. 1. We also assume that a straight coast exists at $y = 0$ and the Coriolis parameter is only a function of y. The two-layer quasi-geostrophic potential vorticity equations are

$$(\partial_t + p_{1x}\partial_y - p_{1y}\partial_x)(\nabla^2 p_1 - p_1 + p_2 + \hat{\beta} y) = 0, \quad (2.1)$$

$$(\partial_t + p_{2x}\partial_y - p_{2y}\partial_x)(\nabla^2 p_2 - \delta^2(p_2 - p_1) + \hat{\beta} y) = 0, \quad (2.2)$$

where p_j ($j = 1$ or 2) represent the geostrophic streamfunctions (geostrophic pressures) in the upper layer and the lower layer, t is time, ∇ is a horizontal differential operator, (∂_x, ∂_y), $\hat{\beta}$ is the y derivative of the Coriolis parameter at the coast and δ^2 is the depth ratio H_1/H_2. These equations have been nondimensionalized by using the scales, $L_R = (\Delta\rho g \rho_0^{-1} H_1)^{1/2} f^{-1}$, for the x, y coordinates, U for the velocity, $\rho_0 f U L_R$ for the pressures and UL_R^{-2} for df/dy. The details of the derivation of these equations can be found in Pedlosky (1979).

Although p_1 for the basic current in the model configuration shown in Fig. 1 is negative, (2.1) and (2.2) are invariable for the transformation of $y \to -y$ and $p_j \to -p_j$. Therefore, results for the present model are also applicable to a current with positive p_1.

b. Weakly nonlinear wave equations

In the present paper, we consider the case in which δ^2 is much smaller than unity, i.e., $H_2 \gg H_1$ and $\hat{\beta}$ is of the order δ^2. In such a situation, since the potential vorticity gradient in the lower layer is of order δ^2, the baroclinic instability can occur only to a disturbance

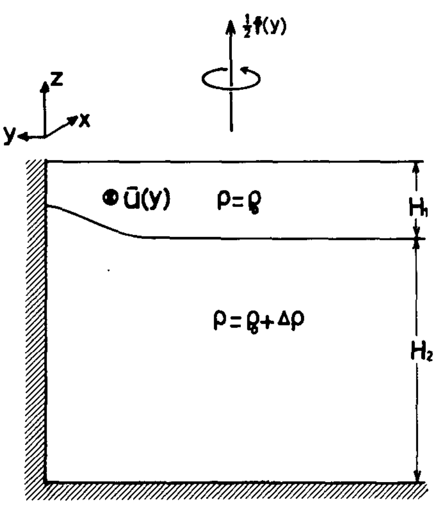

FIG. 1. Model configuration.

whose phase speed is much lower than unity. If we assume the wavelength to be much longer than L_R, we can introduce the new longshore coordinate X and time scale T:

$$X = \delta x, \quad T = \delta^3 t.$$

Assuming the amplitude of the disturbance to be of order δ^2, we expand p_1 and p_2 in powers of δ^2:

$$p_1 = -\int \sum_{n=0}^{\infty} \delta^{2n}\bar{u}_n(y)dy + \sum_{n=1}^{\infty} \delta^{2n}\psi_1^{(n)},$$

$$p_2 = \sum_{n=1}^{\infty} \delta^{2n}\psi_2^{(n)},$$

where $\sum \delta^{2n}\bar{u}_n(y)$ represents the basic current which permits the existence of a longwave with low phase speed, and approaches zero as $y \to -\infty$.

To the lowest order in δ^2, (2.1) and (2.2) become

$$\bar{u}_0(\psi_{1yy}^{(1)} + \psi_2^{(1)})_X - \bar{u}_{0yy}\psi_{1X}^{(1)} = 0 \quad (2.3)$$

$$(\partial_T + \psi_{2X}^{(1)}\partial_y - \psi_{2y}^{(1)}\partial_X)\psi_{2yy}^{(1)} + \beta\psi_{2X}^{(1)} = 0, \quad (2.4)$$

where $\beta = \delta^{-2}\hat{\beta}$. We can easily find that $\psi_2^{(1)} = 0$ is a trivial solution of (2.4). Since our interest is in the coupled motion of the two layers, we set $\psi_2^{(1)}$ to be zero. Then, (2.3) becomes

$$\psi_1^{(1)} = g(y)\phi(X, T),$$

$$g_{yy} - \frac{\bar{u}_{0yy}}{\bar{u}_0} g = 0,$$

$$g = 0 \quad \text{at} \quad y = 0, \quad g \to 0 \quad \text{as} \quad y \to -\infty. \quad (2.5)$$

This equation with the boundary conditions implies that, if $\bar{u}_0$ vanishes at the coast, a stationary longwave solution $g(y) = \bar{u}_0(y)$ exists. Therefore, we assume that the velocity of the basic current at the coast is of order δ^2, i.e., $\bar{u}_0(0) = 0$, and $g(y) = \bar{u}_0(y)$.

To the next order, (2.1) becomes

$$(\bar{u}_{0yy} - \bar{u}_0)\phi_T + (\bar{u}_1\bar{u}_{0yy} - \bar{u}_{1yy}\bar{u}_0 + \beta\bar{u}_0)\phi_X + (\bar{u}_0\bar{u}_{0yyy} - \bar{u}_{0y}\bar{u}_{0yy})\phi\phi_X + \bar{u}_0(\bar{u}_0\phi_{XXX} + \psi_{2X}^{(2)}) = \bar{u}_{0yy}\psi_{1X}^{(2)} - \bar{u}_0\psi_{1yyX}^{(2)}. \quad (2.6)$$

Integrating (2.6) respect to y from $-\infty$ to 0, we get

$$\phi_T + (c_0 + q\phi)\phi_X - r\phi_{XXX} - s\int_{-\infty}^{0} \bar{u}_0\psi_{2X}^{(2)}dy = 0, \quad (2.7)$$

where

$$c_0 = -\left(\bar{u}_{0y}\bar{u}_1|_{y=0} + \beta\int_{-\infty}^{0} \bar{u}_0 dy\right)\Big/ (\bar{Q}(0) - \bar{Q}(-\infty)), \quad (2.8a)$$

$$q = (\bar{u}_{0y})^2|_{y=0}/(\bar{Q}(0) - \bar{Q}(-\infty)), \quad (2.8b)$$

$$r = \int_{-\infty}^{0} \bar{u}_0^2 dy/(\bar{Q}(0) - \bar{Q}(-\infty)), \qquad (2.8c)$$

$$s = 1/(\bar{Q}(0) - \bar{Q}(-\infty)). \qquad (2.8d)$$

In these equations, $\bar{Q}(y)$ is the potential vorticity of the basic current:

$$\bar{Q} = -\bar{u}_{0y} + \int \bar{u}_0 dy. \qquad (2.9)$$

On the other hand, to this order, (2.2) becomes

$$(\psi_{yy} + \bar{u}_0\phi)_T - (\bar{u}_0 - \beta)\psi_X = 0, \qquad (2.10)$$

where the subscript 2 and superscript (2) were dropped for simplicity. The boundary condition at the coast ($y = 0$) is $\psi_X = 0$, and the boundary condition at infinity is that ψ is finite there.

3. Linear stability and nonlinear wave solutions

a. Linear stability and neutral waves

In order to examine the linear stability of the basic flow, we linearize (2.7) and consider a solution of the form

$$(\phi, \psi) = (\hat{\phi}, \hat{\phi}A(y)) \exp[ik(X - cT)], \qquad (3.1)$$

where c is the complex phase speed ($c = c_r + ic_i$). Equations (2.7) and (2.10) become

$$-c + c_0 + rk^2 - s\int_{-\infty}^{0} \bar{u}_0 A dy = 0, \qquad (3.2)$$

$$-c(A_{yy} + \bar{u}_0) - (\bar{u}_0 - \beta)A = 0. \qquad (3.3)$$

Since $\bar{u}_0 \rightarrow 0$ as $y \rightarrow -\infty$, $A(y) \propto \exp[(\beta/c)^{1/2}y]$ for $|y| \gg 1$. When β/c is real and negative, the solution behaves as a Rossby wave at infinity. Otherwise, the boundary condition for A at infinity can be written as $A_y = 0$.

Integrating (3.3) from $y = -\infty$ to 0 after multiplying by the complex conjugate of A and using (3.2), we get

$$1 - \frac{s}{|c|^2}\int_{-\infty}^{0} (\bar{u}_0 - \beta)|A|^2 dy = 0, \qquad (3.4)$$

for $c_i \neq 0$. Since s is $1/(\bar{Q}(0) - \bar{Q}(-\infty))$ and the potential vorticity gradient in the lower layer is $\beta - \bar{u}_0$, this equation implies that the two layers must have opposite gradients of potential vorticity for instability. This condition is, of course, that for baroclinic instability (e.g., see Pedlosky 1979).

From (3.2) and (3.3), we find that when β and $\bar{u}_0(y)$ are specified, c is determined by a single parameter γ:

$$\gamma = c_0 + rk^2. \qquad (3.5)$$

If we consider the limit of $|\gamma| \rightarrow \infty$, $c_0 + rk^2$ in (3.2) balances with c or $s\int_{-\infty}^{0} \bar{u}_0 A dy$. Therefore, at this limit,

$$c = c_0 + rk^2, \qquad (3.6)$$

or

$$c = \frac{\int_{-\infty}^{0} (\bar{u}_0 - \beta)|A|^2 dy}{\int_{-\infty}^{0} |A_y|^2 dy}. \qquad (3.7)$$

Equation (3.6) coincides with the dispersion relation of a shear wave in a one-layer reduced gravity model, while (3.7) represents the phase speed of a longwave in a fluid with potential vorticity gradient of $\beta - \bar{u}_0$ and for this mode $|A| \gg 1$. Since the latter wave is similar to a topographic Rossby wave, we can expect that there are many discrete modes when $\beta/c \geq 0$. For simplicity, we call the former wave U-mode and the latter wave L_n-modes ($n = 1, 2, 3, \cdots$). The instability possibly occurs when the U- and L_n-modes couple.

b. Examples of the dispersion diagram

In order to calculate the phase speed, we must specify the current profile. Since (2.7) and (2.10) do not include terms with y-derivatives of $\bar{u}_0$, the qualitative features are expected to be independent of the detailed structure of $\bar{u}_0(y)$. Then, we assume a simple current profile composed of a piecewise uniform potential vorticity:

$$\bar{Q} = \begin{cases} 0, & \text{for } y < -L \\ 1, & \text{for } 0 > y \geq -L. \end{cases} \qquad (3.8)$$

From (2.9) we obtain

$$\bar{u}_0(y) = \begin{cases} \sinh L \exp(y), & \text{for } y < -L \\ -\sinh y \exp(-L), & \text{for } 0 > y > -L. \end{cases} \qquad (3.9)$$

The coefficients, c_0, q, r and s become

$$c_0 = \bar{u}_1(0)e^{-L} - \beta(1 - e^{-L}), \qquad (3.10a)$$

$$q = e^{-2L}, \qquad (3.10b)$$

$$r = \frac{1}{2}[e^{-L}\sinh L - Le^{-2L}], \qquad (3.10c)$$

$$s = 1. \qquad (3.10d)$$

In this case, $\delta^2\phi$ represents the displacement of the discontinuous surface of potential vorticity (potential vorticity front). The dynamics of the potential vorticity front has extensively been investigated by Pratt and Stern (1986), Stern (1986), etc. In their theories, the strongly nonlinear evolution in a one-layer system was discussed, while the present study deals with the weakly nonlinear dynamics of a two-layer system.

Figure 2 shows the dependence of c on γ for $\beta = 0$, 0.1 and -0.1 with $L = 1$. When $\beta \geq 0$, the U- and L_n-modes couple and the instability occurs within a finite range of γ. One of the critical values of γ which separate stable from unstable waves is zero, and we write the other critical value as γ_c. Since k^2 is positive, this means that the current is stable when c_0 is larger than γ_c. In

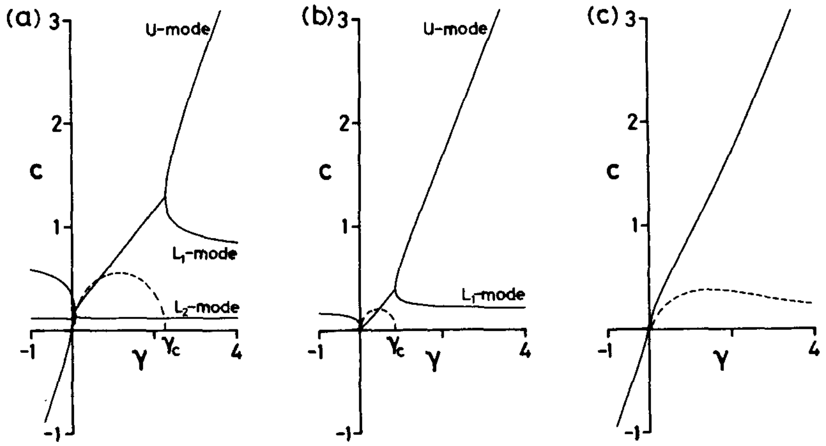

FIG. 2. Real and imaginary parts of the phase speed as a function of γ at (a) $\beta = 0$, (b) $\beta = 0.1$ and (c) $\beta = -0.1$. The solid and the dashed lines denote the real and imaginary parts of c, respectively. γ is $c_0 + rk^2$, the phase speed of the U-mode in the one-layer reduced gravity model. Curves with real c also represent the propagation speeds of solitons and cnoidal waves. In this case, γ is the propagation speed of the nonlinear U-mode in the reduced gravity model and is given in the text [see Eq. (3.13)].

other words, since c_0 is proportional to $\bar{u}_1(0)$, the current with high speed is stable. For positive β, U-mode with negative c does not exist; waves with negative c cannot be trapped near the coast and are radiated as Rossby waves. It follows from (3.4) and (3.7) that if β is larger than the maximum value of $\bar{u}_0$ (=0.432), there is no L_n-mode with positive c and the instability does not occur. On the other hand, for the westward current (i.e., $\beta < 0$) there is no discrete L_n-mode (L_n-mode becomes the continuous Rossby mode), and the current is always unstable. This unstable mode is a radiating mode that is wavy in y and penetrates far into ocean interior (see Talley 1983).

c. Nonlinear wave solutions

Equations (2.7) and (2.10) contains nonlinear wave solutions of the soliton and cnoidal wave. The cnoidal wave solution can be written as

$$\phi = \phi_0 - a\,\mathrm{cn}^2\{k_*^{-1}(aq/12r)^{1/2}(X - cT)\,|\,k_*\}, \quad (3.11a)$$

$$\psi = \phi A(y), \quad (3.11b)$$

where a is the amplitude, ϕ_0 is the value of ϕ at the trough and k_* is the modulus of the Jacobian elliptic function denoted by cn. The wavelength can be written as

$$\lambda = 2k_*(12r/qa)^{1/2}F(k_*),$$

where F is the complete integral of the first kind. Since the zonal average of ϕ_T should be zero [see Eq. (2.7)], ϕ_0 may be chosen as satisfying the relation:

$$\frac{1}{\lambda}\int_0^{\lambda} \phi dX = 0.$$

On the other hand, $A(y)$ and c are determined by (3.3) and

$$c + s\int_{-\infty}^{0} \bar{u}_0 A dy = c_0 + q\phi_0 - \frac{q}{3}a(2 - k_*^{-2}). \quad (3.12)$$

That is, if we set γ to be

$$\gamma = c_0 + q\phi_0 - \frac{q}{3}a(2 - k_*^{-2}), \quad (3.13)$$

the propagation speeds of nonlinear waves are also represented by Fig. 2. However, since the above nonlinear solution is valid only when c is a real number, there is no U-mode cnoidal wave with γ lying between 0 and γ_c, even if the current is linearly stable ($c_0 > \gamma_c$). The amplitudes corresponding to $\gamma = \gamma_c$ and 0 are

$$a_c = \frac{3}{q}(c_0 + q\phi_0 - \gamma_c)(2 - k_*^{-2})^{-1}, \quad (3.14a)$$

$$a_c' = \frac{3}{q}(c_0 + q\phi_0)(2 - k_*^{-2})^{-1}, \quad (3.14b)$$

respectively. Although there is no U-mode solution with an amplitude larger than a_c' when $\beta > 0$, a stationary solution with $a = a_c'$ exists. For this solution, $A(y)$ is zero, and it can also be found from (3.12) and (3.13) that $s\int_{-\infty}^{0} \bar{u}_0 A dy$ is negative for L_n-modes with $a > a_c'$.

If we set k_* to be unity, λ becomes infinity, ϕ_0 vanishes and (3.11a) becomes the soliton solution:

$$\phi = -a\,\mathrm{sech}^2[(aq/12r)^{1/2}(X - cT)]. \quad (3.15)$$

The critical amplitudes for soliton solutions are

$$a_c = \frac{3}{q}(c_0 - \gamma_c), \quad a_c' = \frac{3}{q}c_0. \quad (3.16a,b)$$

Kubokawa (1988) derived a set of coupled equations similar to (2.7) and (2.10) for a coastal current with a surface density front on an f-plane. The above results in the case of $\beta = 0$ are qualitatively the same as those in K88. Therefore, we can expect that nonlinear disturbances on an f-plane in our model behave in a manner similar to those numerically computed by K88. In the present paper, we derive an analytic solution of a disturbance with an amplitude larger than a_c under the linearly stable condition, and discuss the effect of β on the evolution of nonlinear disturbances in eastward currents.

4. Nonlinear growth of a solitary disturbance in a linearly stable current

a. Analytic solution

In order to seek an analytic solution with an amplitude larger than a_c on a linearly stable current, we assume that the amplitude and the value of $c_0 - \gamma_c$ are much smaller than unity and introduce new coordinates with long time and length scales:

$$c_0 - \gamma_c = \epsilon^2\mu, \quad (\phi, \psi) = \sum_{n=1}^{\infty} \epsilon^{n+1}(\phi_n, \psi_n), \quad (4.1)$$

$$\xi = \epsilon(X - c_1 T), \quad \tau = \epsilon^2 T, \quad (4.2)$$

where $c_1 = c(\gamma_c)$ and $\epsilon \ll 1$.

To the lowest order in ϵ, (2.7) and (2.10) become

$$(c_0 - c_1)\phi_{1\xi} - s\int_{-\infty}^{0} \bar{u}_0\psi_{1\xi}dy = 0, \quad (4.3)$$

$$-c_1(\psi_{1yy} + \bar{u}_0\phi_1)_\xi - (\bar{u}_0 - \beta)\psi_{1\xi} = 0. \quad (4.4)$$

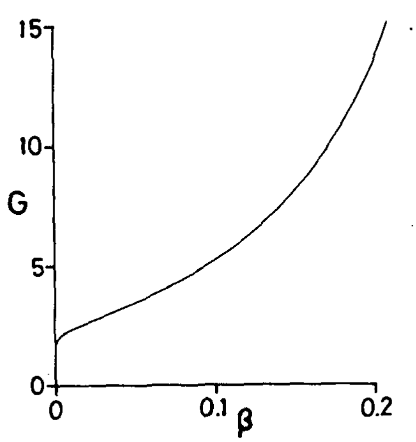

FIG. 3. Value of the coefficient G in (4.13) as a function of β for the current specified by (3.9) with $L = 1$.

These equations imply that we may write

$$\psi_1 = \phi_1(\xi, \tau)A(y). \quad (4.5)$$

To the next order, (2.7) and (2.10) become

$$\phi_{1\tau} + (c_0 - c_1)\phi_{2\xi} - s\int_{-\infty}^{0} \bar{u}_0\psi_{2\xi}dy = 0, \quad (4.6)$$

$$(A_{yy} + \bar{u}_0)\phi_{1\tau} - c_1(\psi_{2yy} + \bar{u}_0\phi_2)_\xi - (\bar{u}_0 - \beta)\psi_{2\xi} = 0. \quad (4.7)$$

From (4.4), (4.5) and (4.7) we can find that for $\phi_{1\tau} \neq 0$,

$$1 - \frac{s}{c_1^2}\int_{-\infty}^{0} (\bar{u}_0 - \beta)A^2 dy = 0. \quad (4.8)$$

This condition is automatically satisfied since $c_1 = c(\gamma_c)$ [see Eq. (3.4)].

To third order in ϵ, (2.7) and (2.10) become

$$\mu\phi_{1\xi} + \frac{q}{2}\phi_{1\xi}^2 - r\phi_{1\xi\xi\xi} + \phi_{2\tau} + (c_0 - c_1)\phi_{3\xi} - s\int_{-\infty}^{0} \bar{u}_0\psi_{3\xi}dy = 0, \quad (4.9)$$

$$(\psi_{2yy} + \bar{u}_0\phi_2)_\tau - c_1(\psi_{3yy} + \bar{u}_0\phi_3)_\xi - (\bar{u}_0 - \beta)\psi_{3\xi} = 0. \quad (4.10)$$

Eliminating ϕ_3 and ψ_3 in (4.9) and (4.10) by the use of (4.3)–(4.8), we obtain

$$\frac{s}{c_1^2}\left[\int_{-\infty}^{0} (\bar{u}_0 - \beta)(\phi_2 A^2 - A\psi_2)dy\right]_{\xi\tau} - \frac{s}{c_1}\phi_{1\tau\tau} + \mu\phi_{1\xi\xi} + \frac{q}{2}\phi_{1\xi\xi}^2 - r\phi_{1\xi\xi\xi\xi} = 0. \quad (4.11)$$

Equations (4.6) and (4.7) imply that we may put

$$\phi_{2\xi} = \chi\phi_{1\tau}, \quad \psi_{2\xi} = B(y)\phi_{1\tau}. \quad (4.12a,b)$$

Then, we get

$$G\phi_{1\tau\tau} - \mu\phi_{1\xi\xi} - \frac{q}{2}\phi_{1\xi\xi}^2 + r\phi_{1\xi\xi\xi\xi} = 0, \quad (4.13)$$

where

$$G = \frac{s}{c_1}\left[1 + \frac{1}{c_1}\int_{-\infty}^{0} (\bar{u}_0 - \beta)A(B - \chi A)dy\right]. \quad (4.14)$$

$B - \chi A$ in (4.14) can be calculated numerically from the following equation, which is obtained from (4.4) and (4.7):

$$(B - \chi A)_{yy} + \frac{(\bar{u}_0 - \beta)}{c_1}(B - \chi A) = -\frac{(\bar{u}_0 - \beta)}{c_1^2}A, \quad (4.15)$$

$$B - \chi A = 0 \quad \text{at} \quad y = 0,$$

$$(B - \chi A)_y \to 0 \quad \text{as} \quad y \to -\infty.$$

From (4.3) and (4.6) we can find that $B - \chi A$ satisfies

$$\int_{-\infty}^{0} \bar{u}_0(B - \chi A)dy = 1/s. \quad (4.16)$$

The value of G is shown in Fig. 3 as a function of β for the current specified by (3.9) with $L = 1$. Here G increases with β, and we can expect that G becomes infinity as β approaches the maximum value of $\bar{u}_0$. Since $\phi_{1\tau} \propto G^{-1/2}$ [see Eq. (4.13)], the evolution is slow when β is large.

If we linearize (4.13) and consider the wavelike perturbation represented by (3.1), we get

$$c = \pm[(\mu + rk^2)/G]^{-1/2}, \quad (4.17)$$

where c is the phase speed on the coordinates defined by (4.2) and the positive and negative signs correspond to the U-mode and L_1-mode, respectively. This equation represent the dispersion relation around $\gamma = \gamma_c$. When μ is positive, i.e., $c_0 - \gamma_c > 0$, the current is linearly stable, and the soliton solutions of U- and L_1-modes exist. Their propagation speeds are

$$c = \pm[(\mu - qa/3)/G]^{1/2}. \quad (4.18)$$

Evidently, their amplitudes should be smaller than $a_c = 3\mu/q$, and from (4.1), we can easily find that $\epsilon^2 a_c$ coincides with that for the soliton in the preceding section. Similar results can also be obtained for the cnoidal wave solution.

On the other hand, a solution with an amplitude larger than a_c was found by Yajima et al. (1983), who studied nonlinear waves in an ion-beam plasma system, using Hirota's method (e.g., see Hirota 1973). The solution can be written as

$$\phi_1 = -\frac{a(1 - \sigma(\tau)\cosh K\xi)}{(\cosh K\xi - \sigma(\tau))^2}, \quad (4.19)$$

where

$$\sigma(\tau) = e^{-\theta}\sinh\left\{\frac{\mu}{(rG)^{1/2}}\left[\frac{a}{4a_c}(1 - a/4a_c)\right]^{1/2}\tau\right\},$$

$$\theta = \frac{1}{2}\ln|(1 - a/4a_c)(1 - a/a_c)^{-1}|,$$

$$K = (qa/12r)^{1/2},$$

$$a_c \leqslant a \leqslant 4a_c.$$

This solution was obtained by considering the interaction between U- and L_1-mode solitons with amplitude $a/4$. Therefore, if we take the limit of $\tau \to -\infty$ in (4.19), the solution separates into two solitons. In other words, disturbances with an amplitude larger than a_c can be produced by the collision of U- and L_1-mode solitons.

At $\tau = 0$, (4.19) takes the same form as the soliton with the amplitude a. For $\tau > 0$, the disturbance grows. When

$$\tau = \frac{(rG)^{1/2}}{\mu}\left[\frac{a}{4a_c}\left(1 - \frac{a}{4a_c}\right)\right]^{-1/2}\ln[e^{\theta} + (e^{2\theta} + 1)^{1/2}], \quad (4.20)$$

$\sigma(\tau)$ becomes 1, and the amplitude becomes infinity. The temporal change of the amplitude [$= -\phi_1$ ($\xi = 0$)] normalized by the initial one is shown in Fig. 4 for various values of a/a_c.

From (4.1), (4.12) and (4.16), we get

$$\int_{-\infty}^{0} \bar{u}_0(\psi - \phi A)_\xi dy = \epsilon^3\phi_{1\tau}\int_{-\infty}^{0} \bar{u}_0(B - \chi A)dy + O(\epsilon^4) = \epsilon^3 s^{-1}\phi_{1\tau} + O(\epsilon^4). \quad (4.21)$$

This equation implies that there is a phase difference between ϕ and ψ for the growing disturbance in which $\phi_{1\tau}$ does not vanish at the peak in ϕ_1 where $\phi_{1\xi} = 0$. That is, the growing disturbance, (4.19), also extracts energy from the potential energy of the basic current in the same manner as the linearly unstable mode.

On the other hand, when $a < a_c$, $\sigma(\tau)$ in the two-soliton solution can be written as

$$\sigma(\tau) = -e^{-\theta}\cosh\left[\frac{\mu}{(rG)^{1/2}}\left\{\frac{a}{4a_c}(1 - a/4a_c)\right\}^{1/2}\tau\right], \quad (4.22)$$

and ϕ_1 is also represented by (4.19). In this case, the U- and L_1-modes cannot couple, and the solution is separating into two solitons with amplitude $a/4$.

b. Numerical results

The analytic solution, (4.19), grows explosively when its initial amplitude is larger than a_c. Since this solution has been derived under the assumption of small amplitude, this asymptotic theory breaks down within a finite time, and in this stage we should return to (2.7) and (2.10). Therefore, we have numerically integrated these equations using a finite difference method, to dis-

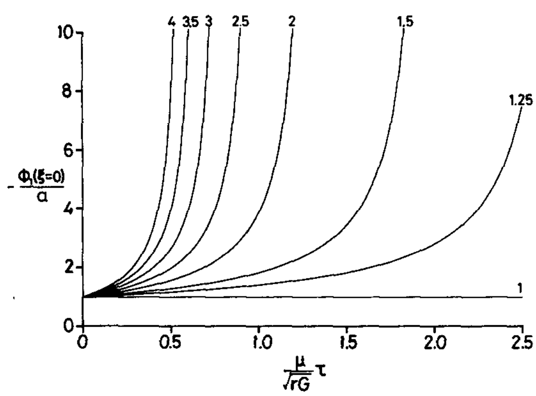

FIG. 4. Temporal change of the amplitude of the growing solution, (4.19). The number attached to each curve denotes the value of a/a_c.

cuss further evolution of the nonlinear growing mode. Since when $\beta = 0$, we have obtained qualitatively the same result as that in K88, we present only the result on a β-plane.

The current profile for numerical computations are taken as the same one considered in section 3b and L is also set to be unity and a cyclic domain in X is adopted. The boundary conditions for ψ are

$$\psi = 0 \quad \text{at} \quad y = 0, \quad \psi_y = 0 \quad \text{at} \quad y = y_L \qquad (4.23)$$

where y_L was set to be -30. In order to remove the effect of the Rossby waves reflected by the offshore boundary, we introduce a bottom friction $-D(y)\psi_{yy}$ on the right-hand side of (2.10), where $D(y)$ has the form

$$D(y) = \begin{cases} 0, & \text{for} \quad y \geq -20 \\ -0.4(20 + y), & \text{for} \quad y < -20. \end{cases} \qquad (4.24)$$

This friction term does not affect disturbances trapped near the coast but damps only the Rossby waves near the offshore boundary.

We consider the initial disturbance of the form

$$\phi = -a \,\mathrm{sech}^2[(aq/12r)^{1/2}X], \quad \psi = \phi A(y), \qquad (4.25)$$

where $A(y)$ is the eigenfunction of the coupled mode at $\gamma = \gamma_c$. The computation has been carried out using the parameters, $\beta = 0.1$ and $c_0 - \gamma_c = 0.1$. In this situation, $a_c = 2.22$ and $a_c' = 21.5$ and we have set the initial amplitude, a, to be 3.33. The results are shown in Figs. 5, 6 and 7. Panels (a) and (b) in Fig. 5 show the evolution of ϕ and ψ at $y = -1$. Figure 6 shows temporal changes of the amplitudes in ϕ and ψ at $y = -1$ and their propagation speeds. In this figure, we also draw the line which represents the change of the amplitude predicted by the analytic solution, (4.19). Figure 7 shows the sequential patterns of the pressure distribution in the lower layer.

From Fig. 5, we find that the disturbance grows as expected from the analytic solution. However, the initial growth rate in the present computation is much smaller than that of the analytic solution (see Fig. 6). The cause of this delay at the initial stage can be attributed to the fact that the phase difference between ϕ and ψ is implicitly assumed in the analytic solution while the initial condition (4.25), has no phase difference. Therefore, the initial adjustment is required before the rapid growth, and this adjustment process causes the delay.

After the amplitude exceeds a_c', the disturbance in ϕ separates from the lower-layer structure, and propagates upstream (westward). When the separation occurs, the lower-layer structure slightly decay but does not alter drastically, and it excites a second disturbance in ϕ. On an f-plane, the large amplitude disturbance after separating from the lower-layer structure propagates as a large amplitude U-mode soliton (see K88). In the present case, there is no U-mode soliton solution whose amplitude is larger than a_c', and the disturbance begins to radiate Rossby waves (Fig. 7). This Rossby wave radiation makes the disturbance decay. Since the propagation speed is a function of its amplitude, as the amplitude decrease its propagation speed approaches zero (Fig. 6). For $T > 31$, it is found that the first disturbance in ϕ turns to grow again and the westward propagation speed increases (Fig. 6). This growth is caused by the interaction with the second disturbance, and we may conclude that if the interaction does not occur, the disturbance approaches the stationary solution with the amplitude a_c'.

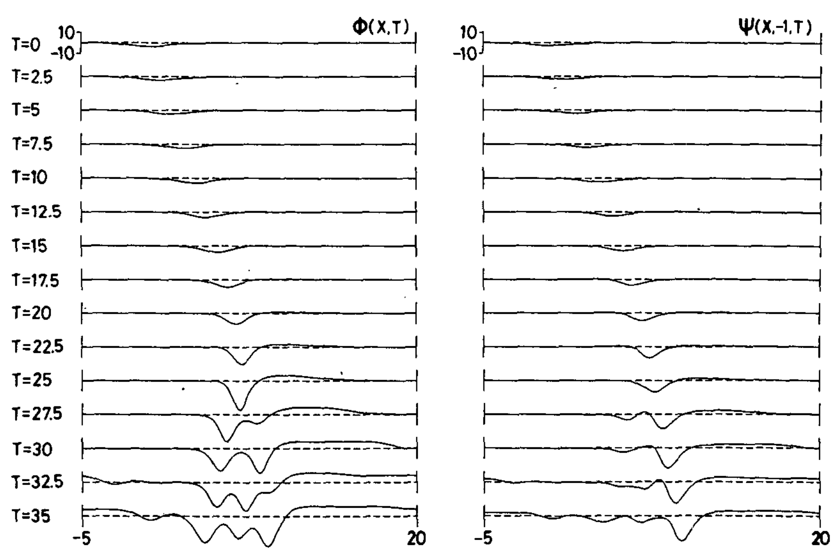

FIG. 5. Temporal evolution of a solitary disturbance on a linearly stable current. $c_0 - \gamma_c$ is 0.1, β is 0.1 and $a/a_c = 1.5$. The left and right panels show $\phi(X, T)$ and $\psi(X, -1, T)$.

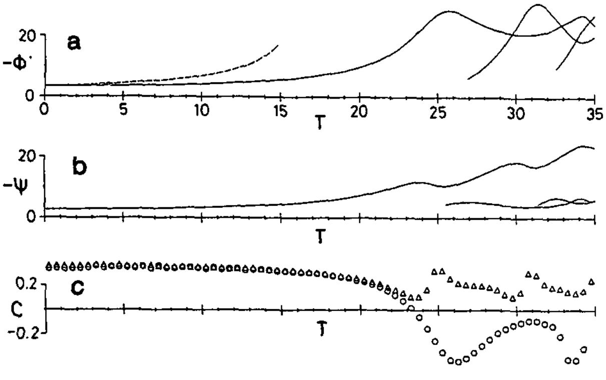

FIG. 6. Temporal changes of the amplitudes in ϕ and ψ at $y = -1$ and their propagation speeds corresponding to Fig. 5: (a) values of ϕ, (b) values of ψ at $y = -1$ and (c) the propagation speeds of the peak in ϕ (circle) and the peak in ψ at $y = -1$ (triangle). The dashed line in panel (a) indicates the change of the amplitude predicted by (4.19).

5. Nonlinear evolution of linearly unstable waves in an eastward current

Coupled equations (2.7) and (2.10) can also describe the nonlinear evolution of linearly unstable modes. In order to treat this problem, we have set the parameter c_0 to be 0.25 in the numerical model used in the preceding section, in which β was set to be 0.1. For this value of c_0, the wavenumber giving rise to the most unstable linear mode is 1.6. First, we consider the evolution of this mode in the cyclic domain of the length $2\pi/1.6$, and the initial amplitude $\hat{\phi}$ in (3.1) was set to be 0.2. In this case, a_c' and ϕ_0 in (3.14b) are 41 and 11.5, respectively, which have been computed numerically by using the equations in section 3c. The results are shown in Figs. 8 and 9.

Figure 8 shows that until the amplitude exceeds a_c', the disturbance grows like that in K88. In K88, it was reported that after the amplitude exceeds a_c', the phase between ϕ and ψ changes and begins to dampen in a manner similar to the damping solution, which is the complex conjugate of the linearly unstable mode, and a large amplitude vacillation was observed. However, in the present case when the amplitude exceeds a_c', Rossby waves are radiated (Fig. 9). This Rossby wave radiation causes the zonal wavenumber in ψ to increase (Figs. 8 and 9), and after that the strong coupling between two layers does not occur. For $T > 20$, the disturbance in ϕ is almost stationary, and its amplitude is about a_c'. The slow eastward propagation and positive pressure in the lower-layer are characters of a L_1-mode cnoidal wave with an amplitude slightly larger than a_c'.

Kubokawa (1988) also examined the nonlinear evolution of an initial disturbance composed of several unstable waves with different wavenumbers and reported that solitary disturbances were produced and the amplitude of each disturbance tended to increase with time while growth and decay were repeated. In order to study a similar problem on the β-plane, we consider an initial disturbance composed of three unstable waves with wavenumbers 1.6/3, 3.2/3 and 1.6. The result is shown in Fig. 10 where the length of the cyclic domain is $6\pi/1.6$ and the initial amplitudes of the three wave components have all been given the same value of 0.2. For this computation, we have set y_L in (4.23) to be -50, since the radiated Rossby waves did not die out and returned to near the coast in a computation with $y_L = -30$.

In the initial stage, each crest grows like the single unstable wave in Fig. 8. Around $T = 14 \sim 16$, the amplitudes exceed a_c' for the most unstable wave.

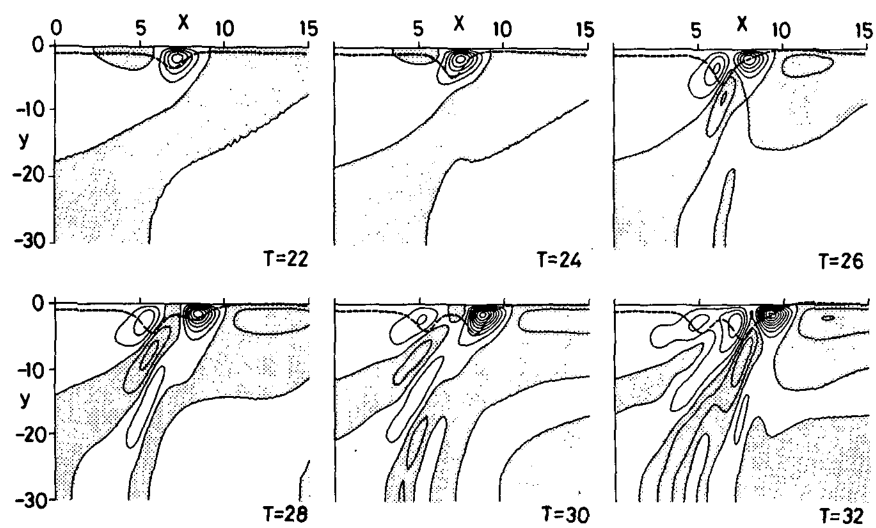

FIG. 7. Sequential patterns of the geostrophic streamfunction in the lower layer, $\psi(X, y)$, corresponding to Fig. 5. The contour intervals are 2.5 and the shadow indicates the region of positive ψ. The dashed lines superposed on the figure represent the distribution of $\phi(X)$.

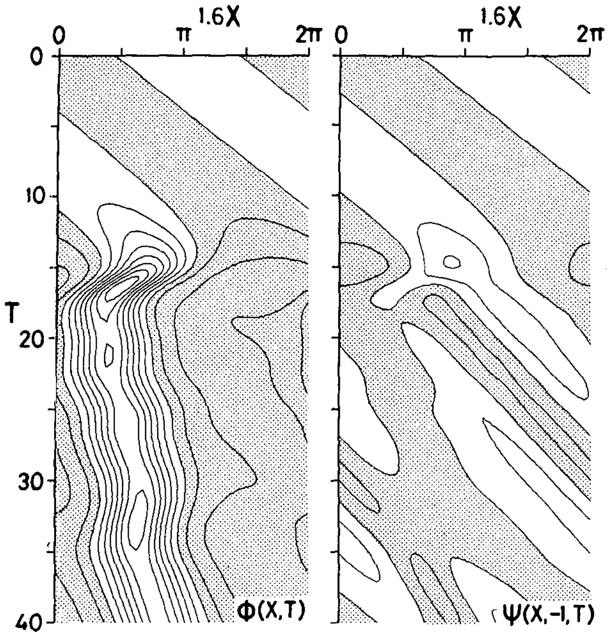

FIG. 8. Temporal evolution of a linearly unstable mode in an eastward current. The initial amplitude is 0.2, c_0 is 0.25 and β is 0.1. The left and right panels show $\phi(X, T)$ and $\psi(X, -1, T)$, respectively. The contour intervals are 5.0 and the shadow indicates the region of positive values.

When the amplitude decreases, a small amplitude U-mode (disturbance in ϕ) appears on the downstream side of the crest in ϕ, and it propagates eastward at a great speed. This type of U-mode also occurred in the case of single unstable wave (Fig. 8), while its amplitude was very small and was not amplified. In the present case, this U-mode interacts with both the disturbances in ϕ and ψ, and its amplitude becomes large. With an increase of crest number, each crest in ϕ tends to be amplified, since a_c' and ϕ_0 are functions of the wavenumber. Although the result is similar to that in K88 in general, the Rossby wave radiation is important in this system, and the propagation speeds of large amplitude disturbances are always small.

For westward currents, unstable waves are radiating modes that penetrate far into ocean interior, and short waves are always unstable. The domain in y in our numerical model is too narrow to compute the evolution of the radiating mode correctly, and the growth of short waves with wavelength comparable to the grid size must be suppressed artificially. Furthermore, a_c' and ϕ_0 for the most unstable linear mode are very large (e.g., $a_c' \approx 190$ and $\phi_0 \approx 60$ for $c_0 = 0$ and $\beta = -0.1$). This seems to suggest that the present weakly nonlinear theory may be inappropriate to discuss the nonlinear evolution of a westward current in the real ocean. For these reasons, we did not carry out any numerical computation on it.

6. Discussion and possible oceanic applications

In the present paper, we have shown that a finite amplitude wave can grow even if the basic current is linearly stable. This result may be applicable to trigger the Kuroshio meander. The Kuroshio is well known as a current which has two remarkable paths; one is a straight path along the southern coast of Japan and the other is a meander path. Each path persists for several years in general. The transition from the straight path to the meander path drastically occurs within three or four months (Shoji 1972; Kawabe 1980). In 1959, 1969 and 1975, it was observed that a small meander that had been generated east of Kyushu propagated eastward, and the Kuroshio took the meander path. The small meander east of Kyushu is thought to be gen-

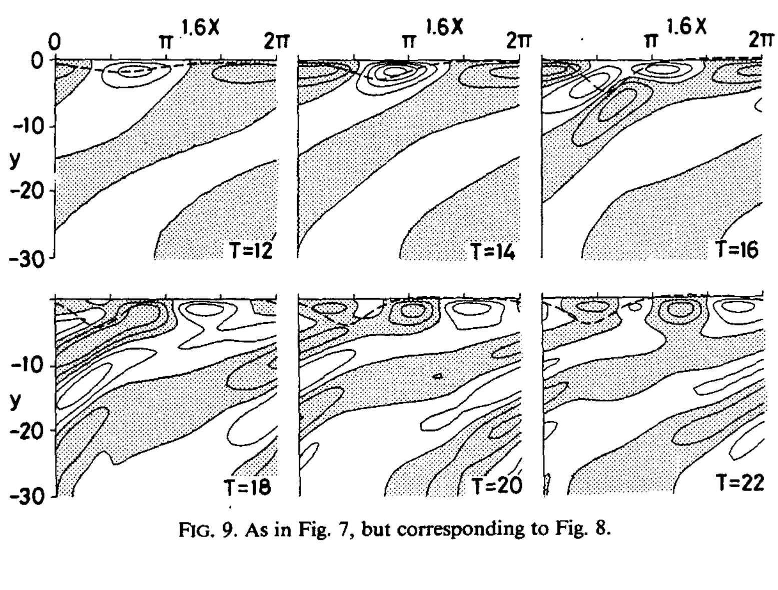

FIG. 9. As in Fig. 7, but corresponding to Fig. 8.

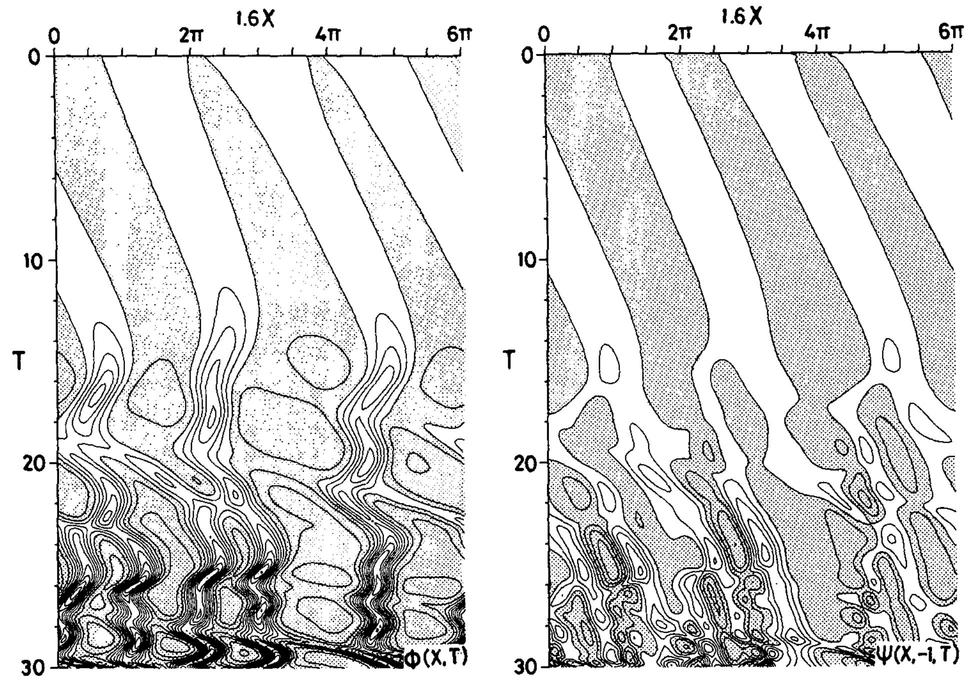

FIG. 10. As in Fig. 8, but the initial disturbance is composed of three unstable waves with wavenumbers 1.6/3, 3.2/3 and 1.6 and the contour intervals are 10.0.

erated by an increase of the Kuroshio velocity (see Sekine and Toba 1981).

Yoon and Yasuda (1987) performed numerical experiments on the Kuroshio path by using a two-layer quasi-geostrophic model. They simulated the above transition process by superposing a upper-layer cyclonic eddy on the current near the western corner of the model ocean (i.e., east of Kyushu) in the case of the straight path. They reported that if the amplitude of the superposed eddy is larger than a certain critical value, it begins to grow, and this growth is sustained by baroclinic energy conversion. These results are consistent with those expected by the present theory.

Yoon and Yasuda also examined the relation between the amplitude necessary for instability and the radius of the superposed eddy, and it was shown that the larger the radius, the smaller the critical amplitude. This result may also be explainable from the present theory. For a system with nonlinear and dispersion terms of the KdV type, when the length scale of the disturbance is small, the dispersion is strong. That is, the initial disturbance with small length scale tends to disperse and amplitude decreases, while a disturbance with large initial scale steepens and its amplitude tends to become large. Therefore, the initial amplitude necessary for instability becomes larger as its length scale becomes smaller.

In dimensional form, time, longshore length, displacement of the current path (the potential vorticity front) and β can be written as

$$t_* = \delta^{-3}L_RU^{-1}T, \quad x_* = \delta^{-1}L_RX, \quad \phi_* = \delta^{-2}L_R\phi,$$
$$\beta_* = \delta^2UL_R{}^{-2}\beta, \tag{6.1}$$

where $\delta^2 = H_1/H_2$ and $L_R = (g'H_1)^{1/2}f^{-1}$. Yoon and Yasuda (1987) assumed that H_1 is 1000 m, H_1/H_2 is $1/3$, $g' = 2 \times 10^{-2}$ m s^{-2}, $f = 7 \times 10^{-5}$ s^{-1} and $\beta_* = 2 \times 10^{-11}$ m^{-1} s^{-1}. These values yield $L_R = 63$ km, and if the nondimensional value of β is set to be 0.1, the maximum current velocity in our model becomes about 1 m s^{-1}, and the nondimensional time required for the initial disturbance to grow to the maximum amplitude in our result corresponds to 40 days in dimensional value. This value is close to the transition time in Yoon and Yasuda's experiment (about 50 days), though the current profile is different from that in their model and the time scale also depends on $c_0 - \gamma_c$ and the initial amplitude. In the real Kuroshio, the transition time seems to be longer than in their experiment. This quantitative difference might arise from the neglect of the bottom slope along the coast.

In our model, the lower-layer structure of the growing disturbance does not decay, and it continues to excite the disturbances in ϕ. Therefore, the stationary meander does not occur, while each disturbance in ϕ tends to be stationary. In the real Kuroshio, the Izu-Ogasawara Ridge exists at the eastern end of the southern coast of Japan, and it will strongly affect the eastward propagating lower-layer structure. If this ridge suppresses further excitation of the disturbance in ϕ, the stationary meander will possibly be established, though the applicability of the present weakly nonlinear theory to the large amplitude meander is uncertain. On the other hand, we have also shown that the propagation speeds of disturbances in ϕ in a linearly unstable eastward current tends to be zero. This tendency might be related to the zero phase speed of large amplitude frontal waves on the Leeuwin Current south of Australia observed by Griffiths and Pearce (1985).

Acknowledgments. The author would like to extend his hearty thanks to Dr. K. Hanawa for fruitful discussion and valuable comments on the manuscript. He is also grateful to anonymous reviewers for their helpful suggestions. This study was partly supported by Grant-in-Aid for Scientific Research from the Ministry of Education, Science and Culture, Japan.

REFERENCES

Flierl, G. R., 1979: Baroclinic solitary waves with radial symmetry. *Dyn. Atmos. Oceans,* **3,** 15–38.

Griffiths, R. W., and A. F. Pearce, 1985: Instability and eddy pairs on the Leeuwin Current south of Australia. *Deep-Sea Res.,* **32,** 1511–1534.

Hirota, R., 1973: Exact *N*-soliton solutions of the wave equation of long wave in shallow water and in nonlinear lattices. *J. Math. Phys.,* **14,** 810–814.

Hukuda, H., 1979: Solitary Rossby waves in a two-layer system. *Tellus,* **31,** 161–169.

Ikeda, M., L. A. Mysak and W. J. Emery, 1984: Observation and modeling of satellite-sensed meanders and eddies off Vancouver Island. *J. Phys. Oceanogr.,* **14,** 3–21.

Kawabe, M., 1980: Sea level variations along the southern coast of Japan and the large meander of the Kuroshio. *J. Oceanogr. Soc. Japan,* **36,** 97–104.

Killworth, P. D., N. Paldor and M. E. Stern, 1984: Wave propagation and growth on a surface front in a two-layer geostrophic current. *J. Mar. Res.,* **42,** 761–785.

Kubokawa, A., 1988: Instability and nonlinear evolution of a density-driven coastal current with a surface front in a two-layer ocean. *Geophys. Astrophys. Fluid Dyn.,* **40,** 195–223.

Long, R., 1964: Solitary waves in westerlies. *J. Atmos. Sci.,* **21,** 197–200.

Pedlosky, J., 1979: *Geophysical Fluid Dynamics.* Springer-Verlag, 624 pp.

Pratt, L. J., and M. E. Stern, 1986: Dynamics of potential vorticity front and eddy detachment. *J. Phys. Oceanogr.,* **16,** 1099–1118.

Redekopp, L. G., 1977: On the theory of solitary Rossby waves. *J. Fluid Mech.,* **82,** 725–745.

Sekine, Y., and Y. Toba, 1981: Velocity variation of the Kuroshio during the small meander south of Kyushu. *J. Oceanogr. Soc. Japan,* **37,** 87–93.

Shoji, D., 1972: The variation of the Kuroshio south of Japan. *Kuroshio: Its Physical Aspects,* H. Stommel and K. Yoshida, Eds., University of Tokyo Press, 127–234.

Stern, M. E., 1986: On the amplification of convergence in coastal currents and the formation of "squirts." *J. Mar. Res.,* **44,** 403–421.

Talley, L. D., 1983: Radiating instabilities of thin baroclinic jets. *J. Phys. Oceanogr.,* **13,** 2161–2181.

Weideman, P. D., and L. G. Redekopp, 1980: Solitary Rossby waves in the presence of vertical shear. *J. Atmos. Sci.,* **37,** 2243–2247.

Yajima, N., M. Kono and S. Ueda, 1983: Soliton and nonlinear explosion modes in an ion-beam plasma system. *J. Phys. Soc. Japan,* **52,** 3414–3423.

Yoon, J. H., and I. Yasuda, 1987: Dynamics of the Kuroshio large meander: two-layer model. *J. Phys. Oceanogr.,* **17,** 66–81.